

# Demonstrating Light Yield and Energy Resolution trends for different sized Scintillators using Monte Carlo Simulations

Contact: adam.illoul@stfc.ac.uk

**A.R.L Illoul**

*School of Physics,  
University of Bristol,  
BS8 1TH, United Kingdom*

**C.D. Armstrong**

*Department of Plasma Physics,  
Central Laser Facility, RAL  
OX11 0QZ, United Kingdom*

## 1 Abstract

Light yield loss due to larger scintillator dimensions has been documented for a number of different scintillators [1] [2]. This was explained using the overlap between the characteristic emission and absorption spectrum of the scintillator - causing self absorption, an effect which rises with respect to the average photon path length. Monte Carlo simulations were used to demonstrate that the increase in surface area of a diffusely reflecting surface wrapped around the scintillator will produce a similar trend, independent of self-absorption. The aspect ratio of two sides of the scintillator was varied to observe its effect on the light yield measured, showing a gradual climb in yield as the ratio increased. There is indication that the detector planes surface area is not driving this increase independently. The energy resolution of scintillators of a given length were established, producing higher resolutions at smaller scintillator lengths. Increased resolution was also found for higher reflection coefficients of the reflective wrapping. A literature comparison is also shown to demonstrate the simulations consistency.

## 2 Introduction

Radiation detection is an important diagnostic component in Laser-plasma physics. Laser-plasma interactions produce a range of ionising particles and photons, the characteristics of which can be used to describe the interaction. These tunable characteristics also allow for non-destructive testing of objects, which is currently in demand in the aerospace and security sector [3]. The ability for Laser driven radiation to repetitively, and promptly probe materials with a controlled spectra allow for a range of densities and thicknesses to be imaged frequently.

One technique to convert the radiation into a readable electronic signal is use scintillators with a photo-detector. Scintillators convert ionising radiation into visible light, and have been used for radiography purposes for interior probing using laser-driven radiation sources [3] [4], gamma/X-ray spectroscopy for laser-plasma diagnostics [5] [6], and are frequently used in the medical industry [7] [8] in PET scans. Two important components of a scintillator are its light yield and energy resolution.

The light yield refers to the efficiency at which the scintillator is able to convert the incident radiation energy into optical light [9]. Using scintillators with a low light yield results in a lower photon emission, which will reduce the reliability of measurement.

The energy resolution measures the consistency at which the scintillator can convert the incident energy. If a single ionising photon is absorbed by the scintillator, the detector will measure an equivalent light response. By repeating this, variations in this response will be observed. This may be due to the emitted optical photons taking different paths within the scintillator, that may include more reflections at the surface - resulting in a lower average amplitude. The scintillators ability to consistently convert the same incident energy into the same amount of optical light determines the precision at which it can measure the incident radiations' energy. This resolution is partly dependent on the light yield, due to the Poissonian nature of photon-counting.

One parameter than contributes towards these two fundamental properties is the dimension of the scintillator used, and is the focus of this report. Using Monte Carlo simulations, the effect of the length of the scintillator on the light yield and energy resolution is observed. Furthermore, the effect of the aspect ratio between two and three dimensions of a scintillator is varied to observe the change in light yield. In the Discussion section, the results are compared to the literature.

## 3 Motivation

High flux X-ray spectrometry can be employed using scintillators. Rusby et. al [6] placed blocks of Bismuth Germanate (BGO) scintillators in a rail-like setup and the light yield was observed orthogonal to the incident radiation, as demonstrated in Fig.1. The crystals are wrapped in Polytetrafluoroethylene (PTFE), which is a reflective coating to improve the optical light yield. By increasing the length (Z-axis dimension) of each block the surface area is increased for the face between the scintillator and the source. For radiation sources that emit spherically, this will result in more X-rays on average being converted into an optical light signal. However, directional X-ray beams [3] would only necessitate the scintillator to encompass the beams cross-section to

observe any gain in signal. Scintillators that are unnecessarily larger in surface area may incur more reflections from the individual photons, and thus become less efficient at converting the radiation into a light signal. The trends of the light yield and energy resolution for different sizes are therefore of importance in producing a reliable light signal for radiation diagnostics.

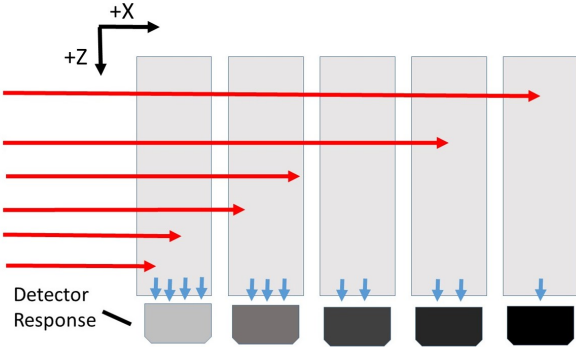


Figure 1: Scintillator based X-ray spectrometer schematic, where the scintillators measured response (blue) to the X-rays (red) dims, the further the X-ray source is from the crystal. An array like the one depicted is coined a 'rail' in the motivation. The coordinates system is referenced throughout the paper, including Y which travels into the page.

#### 4 Theory & Method

The Monte Carlo simulation reproduced the photon transport within a scintillator once the X-ray signal was converted into visible light. The photons are treated as a particle when interacting with the PTFE, with a starting amplitude of 1. We assumed that it is wrapped around homogeneously, so that the reflectance coefficient around the entire scintillator was uniform. The diffuse reflectance of PTFE was implemented on all surfaces except the face imaged by the detector. Typically the reflectance coefficient of PTFE is  $\geq 0.97$  [10] for most scintillators' emission spectrum, but variation is expected for different thicknesses of PTFE, as shown by Janecek [11]. As of such, the range of reflectance coefficients used in the simulation was restricted between 0.95-1.

The face imaged by the detector will transmit and reflect a fraction of the light depending on the angle of incidence - calculated using the Fresnel equations. Additionally, total internal reflection was applied to the simulation. Each of these physical processes are dependent on the refractive index of the two mediums between this face. Generally the scenario observed is where the external medium is air, and this was the case for all simulations except the comparison of Cherry et. al's work [7]. Cherry et. al used optical grease between the scintillator, and the photo-detector, and was therefore implemented into the simulation too. An optical grease refractive index value of 1.5 was used, closely resembling the common market values [12] [13].

X-ray attenuation occurs in the direction at which they travel, and is described by the Beer-Lambert law in Eq.1 illustrating the decay in X-rays that have passed through a medium of length  $l$ . The law takes into account the density  $\rho$  of the medium and the cross-section  $\sigma$  for a photon of given energy.

$$N(l) = N_0 e^{-\rho l \sigma} \quad (1)$$

Two scintillators were used as models; Lutetium-Yttrium Orthosilicate (LYSO) and BGO, the densities of which were sourced from Saint Gobains' data sheets [14] [15]. The cross-section was calculated using NIST's XCOM database [16] attempting to replicate the characteristic 511keV emission from sources such as Na-22.

Using Fig.1's coordinate system as reference, the aspect ratio effect on yield, the height (Y) was varied between 1 – 10mm, while constraining the length (Z) dimension to a value of 10mm, and depth (X) to 2mm. The number of photons simulated was maintained at  $10^5$  particles, as this corresponded to a consistent yield through repetition. The reflectance coefficients of interest were 0.95, 0.97, and 0.99.

The energy resolution was determined by measuring the full-width half-maximum (FWHM) value of a histogram of energy readouts. For each event, 1,500 particles were seeded at a single random point within the scintillator to replicate the physical aspect of energy resolution measurements done by Pepin et. al [17], and the total intensity registered on the detector screen was recorded. This was repeated 10,000 times to produce a distribution of light yields; a pulse height histogram. The characteristics of LYSO were used, where the detector planes immediate external medium is air.

An increase in the length from 10 – 50mm of the scintillator was applied per simulation, and the integrated light yield was determined, with the reflectance coefficient of the reflector 0.95 and 0.97. Finally, the variation in yield and resolution was observed as a function of aspect ratio of the scintillator face upon which the X-rays were incident. To evaluate the simulations competency, a comparison between data from Cherry et.al's work [7] and the simulation was made regarding the trend in light yield as the geometry of the scintillator varied.

#### 5 Results

For a  $2 \times 10$  sized detector plane, a larger length corresponded to a lower light yield as shown in Fig.2. This was fitted with the 2R model (Eq.2). The key parameters LY(0) and  $\mu$  found to fit for each simulation with a given reflectance coefficient is referenced in Table. 1.

$$LY(l) = LY(0) \times \frac{1 - \exp(-2\mu l)_i}{2\mu l} \quad (2)$$

<sup>i</sup>LY( $l$ ) defines the light yield after attenuation through a

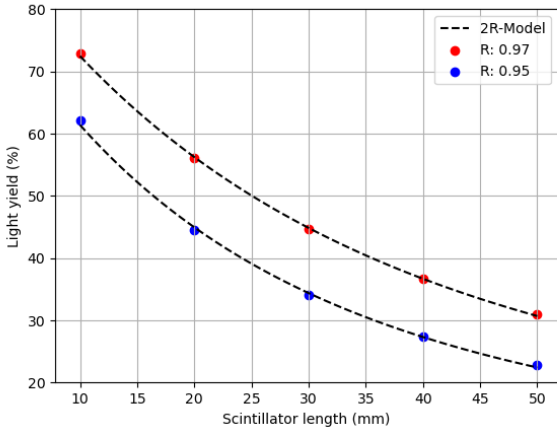


Figure 2: Simulated light yield for a  $2 \times 10 \times Z$  scintillator wrapped in PTFE of reflectivity 0.95 and 0.97, where  $Z$  is the scintillator length. The 2R Model approximation was fitted to the data.

R	LY(0)(%)	$\mu$ ( $\text{mm}^{-1}$ )
0.95	$88 \pm 3$	$3.8 \pm 0.2$
0.97	$96 \pm 1$	$3 \pm 0.06$

Table 1: Values fitted to the Light yield(%) vs Scintillator Length as seen in Fig.2 using the 2R model. Pearson's  $R^2$  were both found to be  $> 0.999$  for the two light yield simulations.

The yield as a function of aspect ratio can be seen in Fig.3, and is the case where all dimensions are constrained except for the  $Y$  (height) axis. A comparison was made to a case where both  $X$  and  $Y$  varied linearly, with a constrained  $Z$  length and is shown in Fig.4. The particle number was kept constant.

A distribution of energy readouts in the form of a Gaussian distribution was found for all lengths of  $Z$ . They were fitted to a Gaussian function, through which the FWHM was calculated. This parameter was plotted for all lengths and reflection coefficients 0.95, 0.97, and 0.99 as seen in Fig.5.

## 6 Discussion

The accuracy of the simulation can be validated by drawing comparisons from literature on light yield. A single source was used to maintain consistency. Cherry et.al [7] measured the light yield for BGO for an array of dimensions, and a comparison can be seen in Fig. 6. The measurements by Cherry, and the simulation's were normalised to the  $3 \times 3 \times 5$  mm<sup>3</sup> scintillator light yield from Cherry. The three sections are divided due to the different dimensions labelled within the plot. The simulations results best fitted these data points with a reflectance coefficient of  $R = 0.92$ . This is likely to be an underestimation of the true reflectance coefficient the experiment

medium of length  $l$ ,  $\mu$  is a loss parameter that includes absorption and scattering. LY(0) is the intrinsic light yield of the scintillator.

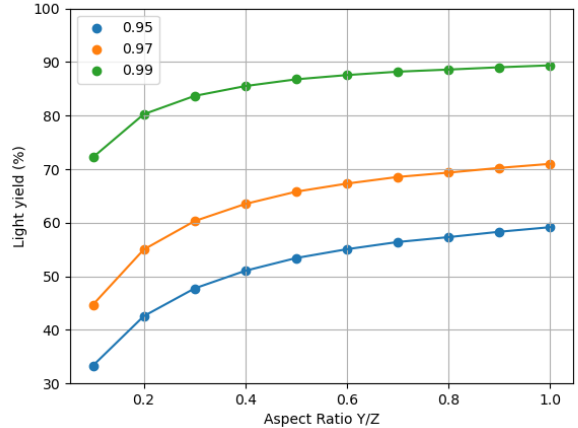


Figure 3: Simulating  $10^5$  particles to produce light yield for different aspect ratios of the scintillator;  $Y/Z$ , where  $Y$  is the height and  $Z$  is the length (orthogonal to the detector face). The length was kept constant at 10, while the height was increased to observe the change in yield.

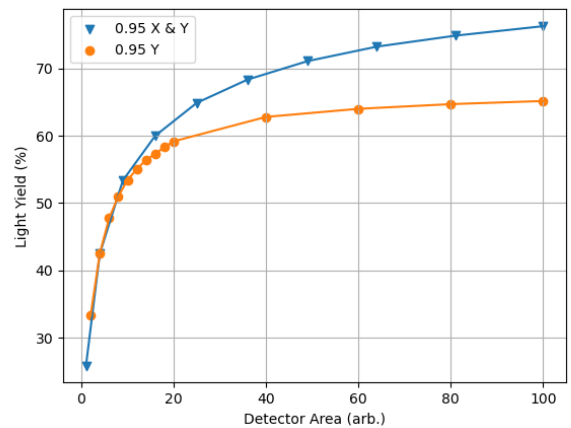


Figure 4: A comparison between the earlier regime in which the  $Y$  was varied, and one in which  $X$  and  $Y$  are varied simultaneously, maintaining a square shaped detector plane. The equivalent areas, yet different yields indicate that the detector plane area is not the driving factor in yield increase. This figure uses the data for the reflectance coefficient 0.95, and a constrained length  $Z = 10$ .

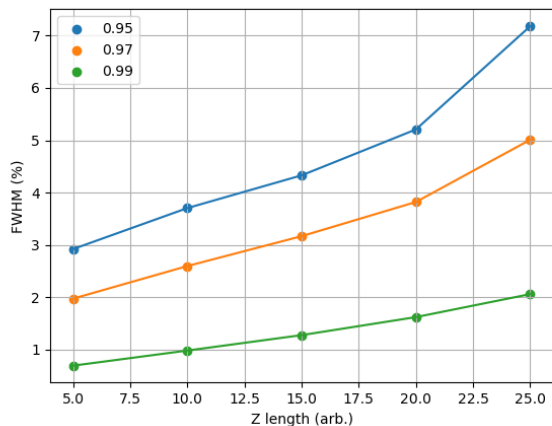


Figure 5: The FWHM of the fitted function from each pulse height histogram as a function of the length of the scintillator for each reflectance coefficient (legend).

had, as stated earlier that typical reflectance coefficients of PTFE are greater than 0.95. The possible sources that cause this may be the untreated self-absorption, a parasitic effect that is caused by the scintillator absorbing its own emission. This would sharpen the descent of the simulations trend with increased length if implemented, and likely reduce the difference seen in Fig.6.

The general decrease in light yield with respect to length found in Fig.2 has been documented in scintillators [7] [18] and is similar to a decrease found by Wojtowicz et. al [1] for LuAP and LuYAP scintillators. However the proposed mechanisms for this loss in the literature is not accounted for in the simulation. Wojtowicz proposed Eq.2 as a model to approximate the light loss due to self absorption, which was accurate at predicting the light yields for lengths 0.1cm and 1cm scintillator lengths, and further studies using the model by Janus et. al [2] for a range of lengths between 0.13cm to 1.02cm. The simulation shows that the model reliably predicts the light yield for lengths between 1-5cm.

The absorption coefficient  $\mu$  as seen in Table.1 is the loss parameter and affects the rate of light loss as the scintillator length is increased. The 2R model has been verified experimentally using LYSO [19], with an absorption coefficient from LYSO of  $0.33\text{cm}^{-1}$ , and so demonstrates the simulations ability to accurately reproduce the trends of light yield as the dimensions are varied.

In our simulation parasitic absorption was neglected due to the model scintillator LYSO's absorption/emission spectra having a minimal overlap, despite being the primary motivation of the 2R-model. Yet a similar trend to the model Wojtowicz proposed is observed. It is put forth that the two properties (self absorption & the diffuse reflectance loss for a given length) coalesce within the loss parameter from Eq.2 in the literature.

With regards to the aspect ratio of the height and

length, an increase in the detector surface area naturally increases the light yield, as the solid angle between the initialisation point of a particle and the detector plane has expanded, increasing the likelihood the photon will travel towards it. This is supported by the gradual climb in yield as the ratio increases. Rusby et. al [6] used a  $2 \times 12$

The ratio of the depth and the height also play a role, as shown in Fig.4. For equivalent surface areas of the detector plane, distinctions can be made between cases where the ratio X/Y are different, indicating that yield is not entirely dependent on the detector plane area alone. While slightly inaccurate to keep the particle number constant when the depth increases, it is not anticipated that any difference would be noted for the light yields found. Large increases in particle number made little to no change on the resulting yield. For example, an increase from  $10^5$  to  $2 \times 10^5$ , the average yield collected over three runs was found to deviate by 0.01%, and was not compensatory for the increase in computation time.

Fig.5 shows that using a more reflective coating and smaller length scintillator reduces the FWHM of the pulse height histogram. Literature values for LYSO describe higher FWHM typically between 8 – 15% [17] [19] [20] for a 662keV source. When subtracting the contributions of the electronic and multiplication noise, Pepin et. al [17] calculated an intrinsic energy resolution of  $2.9 \pm 0.7\%$ . Phunpueok et. al [20] and Yawai et. al [19] completed the same procedure, however produced a much higher intrinsic resolution of 7.5% and 8.2% respectively. However, unlike Pepin's scintillators, they are not of a similar geometry to the ones used in this report, and they do not stipulate the use of a diffuse reflective wrapping. Further work should simulate photon transport for a number of different dimensions and reflection regimes in order to validate the findings of these reports, and establish whether the differences can be entirely explained by the geometry and reflective wrapping alone.

## 7 Conclusion

The simulation demonstrated that light yield as a function of scintillator length can be modelled using the 2R model, and that smaller scintillators are preferable where a high light yield is necessary. The same was true with the energy resolution, which demonstrated a decrease as the scintillator length reduced, however, the reduction of scintillator surface area will reduce the capture rate of spherically emitting radiation, and so a balance is necessary. Increasing both the depth and height of the scintillator simultaneously appeared to increase the light yield significantly higher than when one of these dimensions was increased, indicating that detector area alone cannot be used as a metric for measuring the light yield for varying dimensions.

## References

- [1] A J Wojtowicz et. al. Scintillation light yield of Ce-doped LuAP and LuYAP pixel crystals. *8th International Confer-*

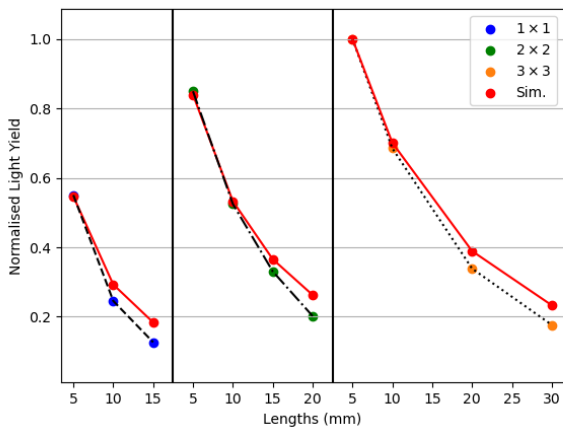


Figure 6: Comparison of the simulations light yield response to the measured light yield by Cherry et. al [7]. The responses are normalised to the  $3 \times 3 \times 5$  light yield sample. The data is best fitted to the simulation data set for reflectance coefficient  $R = 0.92$ .

ence on *Inorganic Scintillators and their Use in Scientific and Industrial Applications*, 2006.

- [2] S Janus et. al. Scintillation light yield of  $\text{BaF}_2:\text{Ce}$ . *Optical Materials*, 31:523–526, 2009.
- [3] C Brenner et. al. Laser-driven x-ray and neutron source development for industrial applications of plasma accelerators. *Plasma Physics and Controlled Fusion*, 58(014039), 2016.
- [4] Chris D Armstrong. Bremsstrahlung radiation and fast electron transport in laser-plasma interactions - Chapter 7. *University of Strathclyde*, 2019.
- [5] R J Clarke et. al. Detection of short lived radioisotopes as a fast diagnostic for intense laser-solid interactions. *Applied Physics Letters*, 89(141117), 2006.
- [6] D R Rusby et. al. Novel scintillator-based x-ray spectrometer for use on high repetition laser plasma interaction experiments. *Rev. Sci. Instrum.*, 89(073502), 2018.
- [7] S R Cherry et. al. Collection of scintillation light from small bgo crystals. *IEEE Transactions on Nuclear Science*, 42(4):1058–1063, 1995.
- [8] Carel W E van Eijk. Inorganic scintillators in medical imaging. *Physics in Medicine and Biology*, 47:R85–R106, 2002.
- [9] G F Knoll. Radiation Detection and Measurement, Third Edition. pages 219–233.
- [10] B K Tsai et. al. A Comparison of Optical Properties between High Density and Low Density Sintered PTFE. *SPIE*, 7065(70650Y-1), 2008.
- [11] M Janecek. Reflectivity spectra for commonly used reflectors. *IEEE Transactions on Nuclear Science*, 59(3), 2012.
- [12] Eljen Technology. Optical grease. <https://eljentechnology.com/products/accessories/ej-550-ej-552>. Accessed 08/21.
- [13] Saint-Gobain. Optical Grease Item BC-631. <https://www.crystals.saint-gobain.com/products/assembly-materials>. Accessed 08/21.
- [14] Saint-Gobain. Lyso datasheet. [https://www.crystals.saint-gobain.com/sites/imdf.crystals.com/files/documents/lyso-material-data-sheet\\_1.pdf](https://www.crystals.saint-gobain.com/sites/imdf.crystals.com/files/documents/lyso-material-data-sheet_1.pdf). Accessed 01/11/20.
- [15] Saint-Gobain. BGO Datasheet. <https://www.crystals.saint-gobain.com/sites/imdf.crystals.com/files/documents/bgo-material-data-sheet.pdf>. Accessed 03/2021.
- [16] National Institute of Standards and Technology. NIST XCOM Database. <https://www.physics.nist.gov/PhysRefData/Xcom/html/xcom1.html>. Accessed: 03/12/20.
- [17] C M Pepin et. al. Properties of lyso and recent lso scintillators for phoswich pet detectors. *IEEE Transactions on Nuclear Science*, 51(3), 2004.
- [18] A Lempicki et. al.  $\text{LuAlO}_3:\text{Ce}$  and other Aluminate Scintillators. *IEEE Transactions on Nuclear Science*, 42(4), 1995.
- [19] N Yawai et. al. Comparison of luminescence, energy resolution and light loss coefficient of  $\text{Gd}_{1.53}\text{La}_{0.47}\text{Si}_2\text{O}_7:\text{Ce}$  and  $\text{Lu}_{1.9}\text{Y}_{0.1}\text{SiO}_5:\text{Ce}$  scintillators. *Nuclear Instruments and Methods in Physics Research A*, 844:129–134, 2017.
- [20] A Phunpueok et. al. Comparison of photofraction for luyap:ce, lyso:ce and bgo crystals in gamma ray detection. *15th International Conference of International Academy of Physical Sciences*, 2012.